2nd International Conference - Water resources and wetlands. 11-13 September, 2014 Tulcea (Romania); Available online at http://www.limnology.ro/water2014/proceedings.html
Editors: Petre Gâștescu ; Włodzimierz Marszelewski ; Petre Bretcan; ISSN: 2285-7923; Pages: 44-50;

SURFACE-GROUNDWATER INTERACTION AND ITS EFFECT ON CARBON CYCLE IN TERRESTRIAL-AQUATIC CONTINUUM

Tadanobu Nakayama, Shamil Maksyutov
National Institute for Environmental Studies (NIES)
16-2 Onogawa, Tsukuba, Ibaraki 305-8506, Japan
E-mail: nakat@nies.go.jp

Abstract
West Siberian Lowland (WSL) contains the world's most extensive peatlands, and also has important influences on hydrologic cycle, provides important role on biogeochemical process, and helps preserve valuable species. In this study, the authors evaluated complex hydrodynamics and their relation to biogeochemical cycles in the WSL by applying advanced process-based model. Though there were a lot of uncertainties about model parameters, the model included reliable values as much as possible from previous studies. The model reproduced reasonably inundated water level due to snowmelt runoff in the lower Ob River in comparison with previous research, and further evaluated connectivity between groundwater and inundated flow affected by complex micro-topography, vegetation, and lithology, which improved the clarification of influence of groundwater on hydrodynamics and biogeochemical process. This simulation system will also play important role in improvement in identification of hot spots of biogeochemical activity and help clarify boundless biogeochemical cycle along terrestrial-aquatic continuum.

Keywords: Boundless Biogeochemical cycle, Eco-hydrology model, Terrestrial-aquatic continuum, West Siberian Lowland.

1 INTRODUCTION

West Siberian Lowland (WSL) contains the world's most extensive peatlands (Smith et al., 2004). In particular, boreal and subarctic peatlands in such as WSL store about 15-30% of the world's soil carbon as sink (Limpens et al., 2008), and affect the dynamics of methane emission as source. Wetlands have also important influences on hydrologic cycle, provides important role on biogeochemical process, and helps preserve valuable species. The WSL includes most of the lower Ob River basin, and is located in permafrost transition (Figure 1). So, the lower Ob, frequently inundated during spring and summer, is different from the middle and the upper Ob in terms of hydrological regime and watershed management. It is important to evaluate eco-hydrological processes there by applying advanced process-based model from the view point of biogeochemical cycle.

2 METHODS

2.1 Process-based NICE model

The original NICE (National Integrated Catchment-based Eco-hydrology) is consisted by complex sub-compartments of surface hydrology model such as hillslope and stream flows, land-surface model including urban and crop process, groundwater model, regional atmospheric model, mass transport model in sediment and nutrient, and vegetation succession model, etc. based on rectangular coordinate after Albers projection or UTM projection (Nakayama, 2008a-b, 2009, 2010, 2011a-b, 2012a-c, 2013, Nakayama&Fujita, 2010, Nakayama&Hashimoto, 2011, Nakayama&Shankman, 2013a-b, Nakayama&Watanabe, 2004, 2006, 2008a-c, Nakayama et al., 2006, 2007, 2010, 2012). The model also includes surface–groundwater interactions assimilating land- surface processes to describe variations of LAI (leaf area index) and FPAR (fraction of photosynthetically active radiation) derived from satellite data. LAI and FPAR are important parameters for evaluating vegetation growth (Nakayama&Watanabe, 2004).

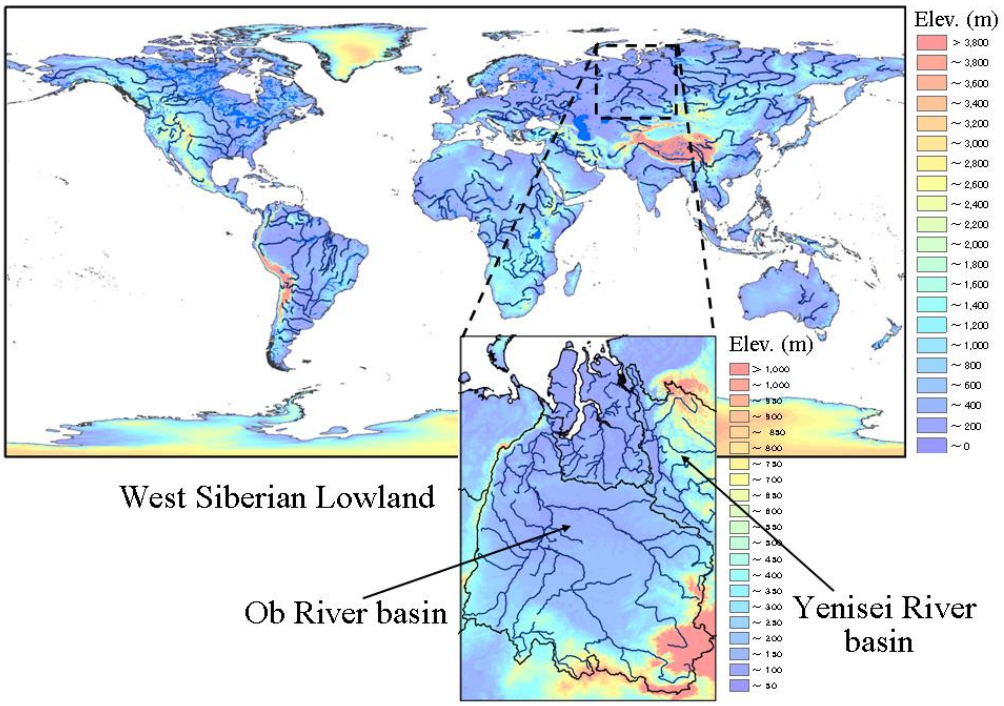

Figure 1. Elevation in the study area of this research (West Siberian Lowland).

2.2 Up-scaling of NICE through coordinate transformation

When we apply NICE to broader area in such as continental or global scale, its application is theoretically limited because it is estimated that curvature in earth and distortion through map projection will increase, in particular, at the corner of projection and at polar zone. So, this application needs the up-scaling of the model, in particular, in horizontal transport components through the implementation of map factor and non-uniform grid in the same way as atmospheric model.

In the case of Mercator's projection, all the metrics in horizontal plane are equal because angles or shapes are preserved there. Therefore, the map factor $m(\phi)$ is calculated in the followings;

$$m(\phi) = \sec\phi \qquad \text{where } x = a\theta,\ y = a\tan\phi = a\ln[\tan(\pi/4+\phi/2)],\ \Delta y = a\sec\phi\Delta\phi \qquad (1)$$

where ϕ and θ are the latitude (°) and longitude (°), a is a radius of the earth, x and y are the length from the projection origin, respectively. This result shows the model has to use non-regular mesh and apply map factor to revise actual length because the distortion Δy and the $m(\phi)$ value increase greatly in the higher latitude (Table 1).

The horizontal transport components in NICE should be converted. The governing equations of NICE about surface hydrology based on kinematic wave theory and groundwater flow based on three-dimensional partial differential equation are described in rectangular coordinate system in the following equations (2) and (3);

$$\frac{\partial Q}{\partial t} + c \cdot \frac{\partial Q}{\partial x'} = c' \cdot r(x', t)\cos\theta'(x') \cdot b'(x') \qquad (2)$$

$$\frac{\partial}{\partial x'}\left(K_{xx}\frac{\partial h_g}{\partial x'}\right) + \frac{\partial}{\partial y'}\left(K_{yy}\frac{\partial h_g}{\partial y'}\right) + \frac{\partial}{\partial z'}\left(K_{zz}\frac{\partial h_g}{\partial z'}\right) + W = Ss\frac{\partial h_g}{\partial t} \qquad (3)$$

where Q = discharge; c' = propagation velocity; r' = effective rainfall intensity; $b'(x')$ = flow width; $\theta'(x')$ = slope angle; h_g = hydraulic potential head; K_{ii} (i=x, y, z) = hydraulic conductivity; W = volumetric flux per

Table 1. Variation of distortion and map factor in 5 (°) x 5 (°) grids.

Lon or Lat	x (m)	Δx (m)	y (m)	Δy (m)	$m(\phi)$
70	7,783,660	555,976	11,056,351	1,458,713	2.9238044
65	7,227,684	555,976	9,597,638	1,207,283	2.36620158
60	6,671,708	555,976	8,390,355	1,036,712	2
55	6,115,732	555,976	7,353,642	914,567	1.7434468
50	5,559,757	555,976	6,439,075	823,833	1.55572383
45	5,003,781	555,976	5,615,242	754,735	1.41421356
40	4,447,805	555,976	4,860,507	701,277	1.30540729
35	3,891,830	555,976	4,159,230	659,594	1.22077459
30	3,335,854	555,976	3,499,636	627,104	1.15470054
25	2,779,878	555,976	2,872,532	602,040	1.10337792
20	2,223,903	555,976	2,270,492	583,179	1.06417777
15	1,667,927	555,976	1,687,313	569,673	1.03527618
10	1,111,951	555,976	1,117,640	560,957	1.01542661
5	555,976	555,976	556,683	556,683	1.00381984
0	0		0		1

unit volume representing sources and/or sinks of water; and S_s = specific storage, respectively. The above equations (2) and (3) are converted by applying map factor in the following;

$$\frac{\partial Q}{\partial t} + c \cdot m(\phi) \frac{\partial Q}{\partial x} = c \cdot r(x,t) \cos\theta(x) \cdot b(x) \tag{4}$$

$$\left(\frac{\partial}{\partial x}\left(m(\phi)^2 K_{xx} \frac{\partial h_g}{\partial x} \right) + \frac{\partial}{\partial y}\left(m(\phi)^2 K_{yy} \frac{\partial h_g}{\partial y} \right) + \frac{\partial}{\partial z}\left(K_{zz} \frac{\partial h_g}{\partial z} \right) \right) + W = Ss \frac{\partial h_g}{\partial t} \tag{5}$$

where $\theta(x)=\tan^{-1}(m(\phi)\Delta Z/L)$; $b(x)= b'(x')/m(\phi)$; and c = the propagation velocity at $\theta(x)$, respectively. In this way, the revised NICE can be applicable to global scale through up-scaling by applying non-uniform grid and map factor into slope angle (topography), flow width, propagation velocity, and hydraulic conductivity.

2.3 Model input data

Six-hour re-analyzed data of downward radiation, precipitation, atmospheric pressure, air temperature, air humidity, wind speed, FPAR, and LAI were input into the model after interpolation of ERA-interim (ECMWF, 2013) in inverse proportion to the distance back-calculated in each grid. Observed meteorological data of BMDS (Baseline Meteorological Data in Siberia) created by the Japan Agency for Marine-Earth Science and Technology (2011) in West Siberia was also used to correct ERA precipitation data because the global ECMWF precipitation sometimes had the least reliability and underestimated observed peak values (Nakayama, 2011a-b, 2012c, Nakayama&Shankman, 2013a-b, Nakayama&Watanabe, 2008b, Nakayama et al., 2006). Mean elevation was calculated by using a global digital elevation model (DEM; GTOPO30) (U.S. Geological Survey, 1996a). In West Siberia wetland, 161 stream channels were selected out from river network data (HYDRO1K) (U.S. Geological Survey, 1996b) by evaluating Pfafstetter level and Strahler stream order and previous materials (Mean river width for lower Ob = 2 km, Biancamaria et al., 2009; Main Ob's channel = 3 km, Kouraev et al., 2004). Though there were a lot of uncertainties about model parameters, the

model included reliable values as much as possible from previous studies, for example, the river width mentioned in the above, and peat depth (Kremenetski et al., 2003, Smith et al., 2004, National Snow and Ice Data Center, 2004). Land cover was categorized on the basis of Global Land Cover 2000 (European Commission, 2013). Though there were a lot of uncertainties about model parameters in West Siberia wetland, the model included reliable values as much as possible from other valuable information such as peat type, peat depth, and geology, etc. was used from West Siberian Lowland Peatland GIS Database (National Snow and Ice Data Center, 2013). The geological structures were divided into four types on the basis of hydraulic conductivity, the specific storage of porous material, and specific yield based on the previous materials. These model parameters of hydrologic and ecological characteristics, soil and vegetation properties, and geological structures were calibrated by comparison between simulated and observed values within the initial estimated known range and published in the literature (Clapp&Hornberger, 1978, Rawls et al., 1982).

2.4 Boundary conditions and running simulation

At the upstream boundaries, reflecting condition on hydraulic head was used assuming that there is no inflow from the mountains in the opposite direction. In the hillslope hydrology, flow depth and discharge at the uppermost ridges of the mountains were set to zero throughout the simulation. Inflows or outflows from the riverbeds were simulated at each time step depending on the difference in the hydraulic heads of groundwater and river. At sea boundary, constant head was set at 0 m. Details are described in Nakayama&Watanabe (2004).

In the West Siberia wetland, the simulation was conducted in horizontally about 2100 km wide by 3000 km long with a resolution of 10 km and 0.15 ° (Figure 1), and the area was discretized into 20 layers with a weighting factor of 1.1 layers (finer at the upper layers) in the vertical direction. The upper layer was set at 2 m depth, and the 20th layer was defined as an elevation of –200 m from the sea surface. Simulations were performed with a time step of Δt = 6 h for 1998-1999 after 1 year of warm-up period until equilibrium. The simulated results were calibrated and validated in hydrologic, geomorphic, and ecological aspects respectively in the author's previous researches (Nakayama, 2008a-b, 2009, 2010, 2012b, 2013, Nakayama&Watanabe, 2004, 2006). Then, the simulated results before and after coordinate transformations were compared with each other and then up-scaled to the global scale with a resolution of 1.0 °.

3 RESULTS AND DISCUSSIONS

3.1 Impact of coordinate transformation on eco-hydrological processes

The simulated result after coordinate transformation into longitude-latitude coordinate system was compared with the original one in rectangular coordinate system in the WSL (Figure 2). The simulated groundwater level after the coordinate transformation (Δx = 0.15 °) reproduces reasonably the spatial characteristics of hydrologic cycle in comparison with the original one (Δx = 10 km) in the island scale in the same way as river discharge though there are some discrepancy at the upstream of Ob River and the downstream Yenisei River because of the slight difference in boundary conditions. NICE can simulate not only groundwater but also surface water because the model includes surface–groundwater interaction in addition to geomorphic change and vegetation succession processes (Nakayama, 2008a-b, 2009, 2010, 2011a-b, 2012a-c, 2013, Nakayama&Fujita, 2010, Nakayama&Hashimoto, 2011, Nakayama&Shankman, 2013a-b, Nakayama&Watanabe, 2004, 2006, 2008a-c, Nakayama et al., 2006, 2007, 2010, 2012). This interaction becomes complicated in the West Siberian Lowland where almost flat region expands, shallow aquifer flows, and continuous and discontinuous permafrost exists heterogeneously. NICE includes various subcompartments to simulate these hydrodynamics iteratively.

3.2 Evaluation of inundated flow in the lower Ob

Figure 3 shows inundated flow in the lower Ob River in July 1998 (spring snowmelt season) simulated by NICE. The model reproduced reasonably inundated water level due to snowmelt runoff there in comparison with the previous research estimated by multisatellite approach (Frappart et al., 2010), and fur-

ther clarified connectivity between groundwater and inundated flow, which improved the clarification of nonlinear interaction in previous study (Reeve et al., 2000). Though the model reproduced reasonably the observed value there, it is necessary to clarify the effect of different latitude on hydrologic change in the future because the distortion and the map factor increase in the higher latitude, which revise to preserve the governing equations through coordinate transformation as a first approximation. From the view point of the role of inland water on biogeochemical cycle where the patterns in surface water CO_2 in stream networks have been seldom explored (Teodoru et al., 2009), first-order streams, the smallest streams that typically appear on mountainous regions, contribute the largest proportion of the CO_2 efflux to the atmosphere (Butman&Raymond, 2011), which implies we have to choose the best resolution depending on the final objective. This result indicates the effectiveness of up-scaling and converting of governing equations of NICE by applying map factor and non-uniform grid, which can be applicable to global scale.

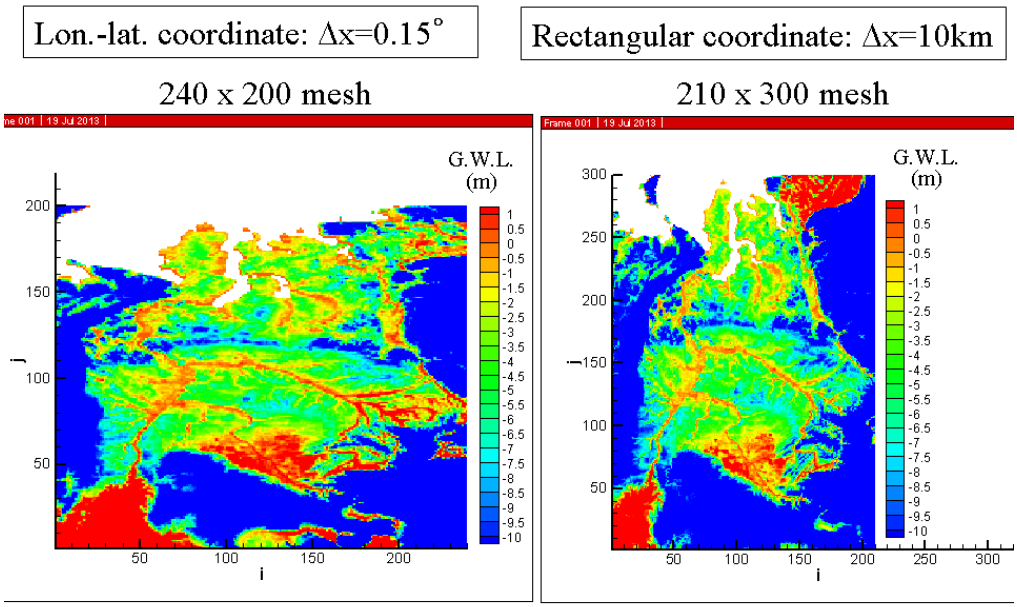

Figure 2. Comparison of simulated G.W.L. relative to the ground surface through coordinate transformation.

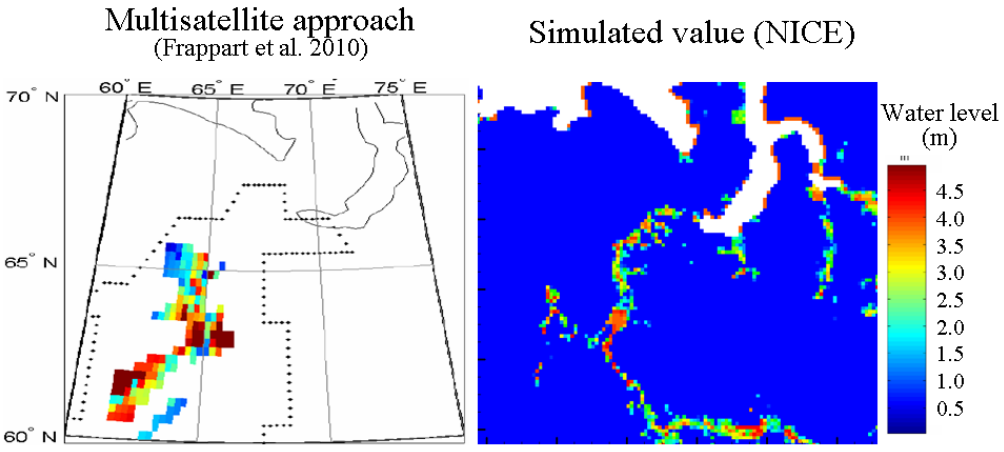

Figure 3. Comparison of inundated water level in the lower Ob River basin (July 1998).

4 CONCLUSIONS

The revised NICE (National Integrated Catchment-based Eco-hydrology) in this study further shed light on the extension of applying this model from local/regional scale to global scale. The model repro-

duced reasonably the surface water – groundwater interaction at the lower altitude regions and showed the possibility of expansion to the global eco-hydrological process.

REFERENCES

Biancamaria, S. et al. 2009, Large-scale coupled hydrologic and hydraulic modelling of the Ob river in Siberia, *J. Hydrol.,* **379**, 136-150, doi:10.1016/j.jhydrol.2009.09.054.

Butman, D. & Raymond, P.A. 2011, Significant efflux of carbon dioxide from streams and rivers in the United States, *Nat. Geosci.,* **4**, 839-842.

Clapp R.B. & Hornberger G.M. 1978, Empirical equations for some soil hydraulic properties, *Water Resour. Res.*, **14**, 601–604.

European Centre for Medium-Range Weather Forecasts (ECMWF) 2013, *ERA-Interim,* http://data-portal.ecmwf.int/data/d/interim_daily/.

European Commission 2013, *Global Land Cover 2000,* http://bioval.jrc.ec.europa.eu/products/glc2000/products.php.

Frappart, F. et al. 2010, Interannual variations of the terrestrial water storage in the Lower Ob' basin from a multisatellite approach, *Hydrol. Earth Syst. Sci.,* **14**, 2443-2453, doi:10.5194/hess-14-2443-2010.

Japan Agency for Marine-Earth Science and Technology 2011, *Baseline Meteorological Data in Siberia (BMDS) Version 5.0.*

Kouraev, A.V. et al. 2004, Ob' river discharge fromTOPEX/Poseidon satellite altimetry (1992-2002), *Remote Sens. Environ.,* **93**, 238-245, doi:10.1016/j.rse.2004.07.007.

Kremenetski, K.A. et al. 2003, Peatlands of the Western Siberian Lowlands: current knowledge on zonation, carbon content and late Quaternary history, *Q. Sci. Rev.,* **22**, 703-723.

Limpens, J. et al. 2008, Peatlands and the carbon cycle: from local processes to global implications ? a synthesis, *Biogeosciences,* **5**, 1475-1491.

Nakayama, T. & Watanabe, M. 2004, Simulation of drying phenomena associated with vegetation change caused by invasion of alder (Alnus japonica) in Kushiro Mire, *Water Resour. Res.,* **40(8)**, W08402, doi:10.1029/2004WR003174.

Nakayama, T. & Watanabe, M. 2006, Simulation of spring snowmelt runoff by considering micro-topography and phase changes in soil layer, *Hydrol. Earth Syst. Sci. Discuss.,* **3**, 2101-2144.

Nakayama, T. et al. 2006. Simulation of groundwater dynamics in North China Plain by coupled hydrology and agricultural models, *Hydrolol. Process.,* **20(16)**, 3441-3466, doi:10.1002/hyp.6142.

Nakayama, T. et al. 2007, Effect of underground urban structures on eutrophic coastal environment., *Sci. Total Environ.,* **373(1)**, 270-288, doi:10.1016/j.scitotenv.2006.11.033.

Nakayama, T. 2008a, Factors controlling vegetation succession in Kushiro Mire, *Ecol. Model.,* **215**, 225-236, doi:10.1016/j.ecolmodel.2008.02.017.

Nakayama, T. 2008b, Shrinkage of shrub forest and recovery of mire ecosystem by river restoration in northern Japan, *Forest Ecol. Manag.,* **256**, 1927-1938, doi:10.1016/j.foreco.2008.07.017.

Nakayama, T. & Watanabe, M. 2008a, Missing role of groundwater in water and nutrient cycles in the shallow eutrophic Lake Kasumigaura, Japan, *Hydrol. Process.,* **22**, 1150-1172, doi:10.1002/hyp.6684.

Nakayama, T.& Watanabe, M. 2008b, Role of flood storage ability of lakes in the Changjiang River catchment, *Global Planet. Change,* **63**, 9-22, doi:10.1016/j.gloplacha.2008.04.002.

Nakayama, T. 2010, Simulation of hydrologic and geomorphic changes affecting a shrinking mire, *River Res. Applic.,* **26(3)**, 305-321, doi:10.1002/rra.1253.

Nakayama, T. & Fujita, T. 2010, Cooling effect of symbiotic urban pavements made of new materials on water and heat budgets, *Landscape Urban Plan.,* **96**, 57-67, doi:10.1016/j.landurbplan.2010.02.003.

Nakayama, T. et al. 2010, Simulation of water resource and its relation to urban activity in Dalian City, Northern China, *Global Planet. Change,* **73**, 172-185, doi:10.1016/j.gloplacha.2010.06.001.

Nakayama, T. 2011a, Simulation of the effect of irrigation on the hydrologic cycle in the highly cultivated Yellow River Basin, *Agr. Forest Meteorol.,* **151**, 314-327, doi:10.1016/j.agrformet.2010.11.006.

Nakayama, T. 2011b, Simulation of complicated and diverse water system accompanied by human intervention in the North China Plain, *Hydrol. Process.,* **25**, 2679-2693, doi:10.1002/hyp.8009.

Nakayama, T. & Hashimoto, S. 2011, Analysis of the ability of water resources to reduce the urban heat island in the Tokyo megalopolis, *Environ. Pollut.,* **159**, 2164-2173, doi:10.1016/j.envpol.2010.11.016.

Nakayama, T. 2012a, Visualization of missing role of hydrothermal interactions in Japanese megalopolis for win-win solution, *Water Sci. Technol.,* **66(2)**, 409-414, doi:10.2166/wst.2012.205.

Nakayama, T. 2012b, Feedback and regime shift of mire ecosystem in northern Japan, *Hydrol. Process.*, **26(16)**, 2455-2469, doi:10.1002/hyp.9347.
Nakayama, T. 2012c, Impact of anthropogenic activity on eco-hydrological process in continental scales, *Proc. Environ. Sci.*, **13**, 87-94, doi:10.1016/j.proenv.2012.01.008.
Nakayama, T. et al. 2012, Multi-scaled analysis of hydrothermal dynamics in Japanese megalopolis by using integrated approach, *Hydrol. Process.*, **26(16)**, 2431-2444, doi:10.1002/hyp.9290.
Nakayama, T. 2013, For improvement in understanding eco-hydrological processes in mire, *Ecohydrol. Hydrobiol.*, **13**, 62-72, doi:10.1016/j.ecohyd.2013.03.004.
Nakayama, T. & Shankman, D. 2013a, Impact of the Three-Gorges Dam and water transfer project on Changjiang floods, *Global Planet. Change*, **100**, 38-50, doi:10.1016/j.gloplacha.2012.10.004.
Nakayama, T. & Shankman, D. 2013b, Evaluation of uneven water resource and relation between anthropogenic water withdrawal and ecosystem degradation in Changjiang and Yellow River basins, *Hydrol. Process.*, **27(23)**, 3350-3362, doi:10.1002/hyp.9835.
National Snow and Ice Data Center 2004, *West Siberian Lowland Peatland GIS Database*, http://nsidc.org/data/arcss131.html.
Rawls, W.J. et al. 1982, Estimation of soil water properties, *Trans. ASAE*, **25**, 1316–1320.
Reeve, A.S. et al. 2000, Simulating vertical flow in large peatlands, *J. Hydrol.*, **227**, 207-217.
Smith, L.C. et al. 2004, Siberian peatlands a net carbon sink and global methane source since the Early Holocene, *Science*, **303**, 353-356.
Teodoru, C.R. et al. 2009, Patterns in pCO2 in boreal streams and rivers of northern Quebec, Cananda, *Global Biogeochem. Cy.*, **23**, GB2012, doi:10.1029/2008GB003404.
U.S. Geological Survey (USGS) 1996a, *GTOPO30 Global 30 Arc Second Elevation Data Set*, USGS, http://www1.gsi.go.jp/geowww/globalmap-gsi/gtopo30/gtopo30.html.
U.S. Geological Survey (USGS) 1996b, *HYDRO1K*, USGS, https://lta.cr.usgs.gov/HYDRO1K.